LOCAL HEAT TRANSFER COEFFICIENTS IN A RECTANGULAR DUCT WITH PLATE BLOCKAGES OF VARIABLE STREAMWISE SPACING

M. Molki and I. Mirzaee
Department of Mechanical Engineering
Isfahan University of Technology
Isfahan, Iran

Abstract An experimental investigation is conducted to determine the effect of repeated-plate blockages of variable streamwise spacing on heat transfer characteristics of turbulent flow in rectangular ducts. The plates are attached to the upper and lower walls in a staggered arrangement. The experiments are carried out by mass transfer and the analogy between heat and mass transfer provides the necessary link between the two processes. The study encompasses both the developing and the periodically fully-developed portions of the duct, and the axial distribution of the local transfer coefficients are discussed. The principal variables of the problem are Reynolds number Re, plate height h, and plate streamwise spacing L. The range of Re, h/H (H= duct height), and L/H considered in this study are 3000-50000, 0-0.5, and 1-7. The measurements extended downstream to about 13 duct hydraulic diameter.

Key Words Heat Transfer, Rectangular Duct, Blockage, Turbulent Flow, Mass Transfer, Local Coefficient, Reynolds Number

چکیده دراین بررسی تجربی، اثر موانع پره ای متعدد و تغییر فاصلهٔ آنها بر ویژگیهای حرارتی جریان مغشوش در کانالهای مستطیلی مورد توجه قرار گرفته است. آزمایشها از طریق انتقال جرم اجرا شده اند و تشابه پدیده های انتقال جرم و حرارت ارتباط لازم میان دو فرایند را فراهم کرده است. دراین مقاله، نواحی توسعه یافته درحال توسعهٔ کانال هردو موردنظر قرار گرفته اند و توزیع ضرایب موضعی انتقال ارائه شده است. پارامترهای اصلی مسئله عبارتند از عدد رینولدز Re، ارتفاع پره h و فاصلهٔ پره ها در امتداد جریان L. گسترهٔ تغییرات Re، h/H (H= ارتفاع مقطع کانال) و L/H به ترتیب ازاین قرارند: ۳۰۰۰ تا ۵۰۰۰، ۰ تا ۰/۵ و ۱ تا ۷. اندازه گیری میزان انتقال جرم تا فاصلهٔ ۱۳ برابر قطر هیدرولیکی مجرا به سوی پائین جریان انجام شده است.

INTRODUCTION

Plate blockages are often installed in flow passages to promote turbulence and thereby to enhance heat transfer. One possible arrangement for the plates is to deploy them along the upper and lower walls of the duct in a staggered manner, so that the zigzag path thus provided for the flow would encourage the fluid to separate behind the plates and occasionally to impinge upon the duct walls. The combined action of flow separation and repeated wall impingements would increase turbulence and flow mixing, which in turn would improve the heat transfer characteristics of the flow field.

A search in the literature has revealed a limited number of available related studies. The experimental investigations of Berner et al. [1] and those conducted by Sparrow and Wachtler [2], and the numerical studies of Webb and Ramadhyani [3] and those of Kelkar and Patankar [4] have provided some insight into the problem. There are, however, some limitations to the previous investigations. While Reference [1] addressed the fluid mechanics aspects of the problem, References [3 and 4] were confined to the domain of laminar flow with its rather limited practical application.

The present work concerns an experimental effort to investigate the transfer characteristics of turbulent flow in a rectangular duct with repeated-plate blockages. A simplified side view of the internal geometry of the duct is shown in Figure 1. As seen in the figure, the plate blockages have a staggered arrangement.

The internal geometry of the duct is determined by several dimensional parameters. These parameters are: 1) duct height, H, 2) duct width, W, 3) plate height, h, and 4) plate spacing, L. When expressed in dimensionless form, these parameters reduce to W/H (aspect ratio), h/H and L/H. In addition to these geometric parameters, the flow Reynolds number, Re, and streamwise distance along the

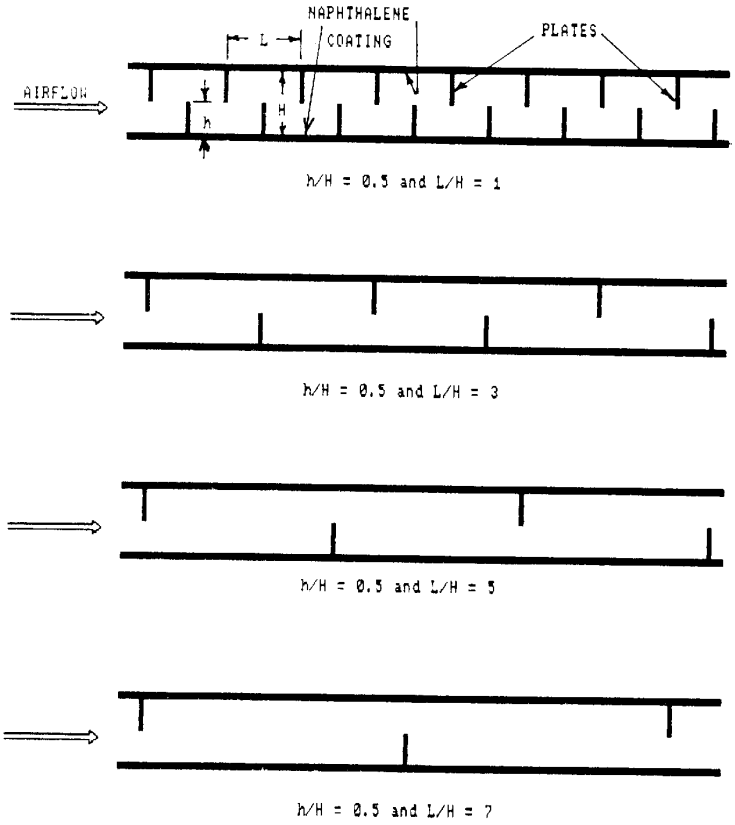

Figure 1. Schematic side view of the duct.

duct in distance-to-hydraulic-diameter form, x/D_h, are also important. In this work, the aspect ratio was fixed at W/H= 4, while h/H, L/H, Re, and x/D_h ranged, respectively, from 0-0.5, 1-7, 3000-50000, and 0.34-12.81.

In this investigation, the heat transfer problem was simulated by a mass transfer model. The experiments were carried out via mass transfer and the well-established analogy between heat and mass transfer provided the necessary link between the two problems. The particular mass transfer method employed here is the well-known naphthalene sublimation technique. The validity of this particular technique for predicting heat transfer has been experimentally proved by many investigators, including those of Reference [5]. The theortical basis for the analogy is discussed by Eckert [6].

Experimental Setup and Procedure

The main element of the experimental setup is the flow duct. The schematic side view of the duct is shown in Figure 1. The plate blockages were made of 0.75 mm galvanized sheet metal and were installed on the upper and lower walls in a staggered arrangement.

The duct had a rectangular cross-section (width W= 6.0 cm x height H= 1.5 cm) and was of such a length to permit the measurements to be carried out downstream to x= 31 cm. The upper and lower walls had a modular design, so that each module could be removed from the test section for mass measurements.

A total of 40 naphthalene-coated aluminum modules (20 on each wall with the arrangement seen in Figure 1) were employed in the experiments. Prior to each data run, the aluminum modules were placed inside a special mold, and they were individually cast by pouring molten naphthalene into the mold. The casting was performed against a highly smooth surface and therefore the naphthalene surface was also smooth. The naphthalene-coated modules were kept in a laboratory overnight to attain thermal equilibrium. Mass transfer experiments typically last 15 minutes to 2 hours, depending on the flow rate.

The modular design of the duct not only permitted a local measurement of transfer coefficients along the duct, but it also permitted a systematic variation of the plate-spacing L. As shown in Figure 1, the dimensionless plate spacing was L/H= 1,3,5 and 7, corresponding respectively to 1,3,5, and 7 naphthalene modules located between each pair of neighboring plates. The exact location of the plate blockages are given in Table 1.

The mass transfer experiments were initiated by turning on a centrifugal fan and thereby drawing the laboratory air into the duct. During each data run, the air temperature was recorded several times at the inlet of the duct by a mercury thermometer with a resolution of 0.25 C. To determine the rate of mass sublimation at each axial station along the duct, the modules were individually weighed on a balance before and after each data run, and the mass changes were determined to within 0.1 mg. The mass changes were typically around 15 mg.

The air-flow rate was measured by an orifice plate which was situated downstream from the test section. The orifice plate had been calibrated before, and it was determined that the orifice discharge coefficient was CD= 0.5979 ± 0.0226 [5].

Data Reduction

The mass transfer coefficient for the *i* th module was

TABLE 1. Values of Streamwise Coordinate, x/D_h, for Plate Locations

	x_{plate}/D_h			
Plate no.	L/H= 1	L/H= 3	L/H= 5	L/H= 7
1	0.653	0.653	0.653	0.653
2	1.307	-------	-------	-------
3	1.960	-------	-------	-------
4	2.613	2.613	-------	-------
5	3.266	-------	-------	-------
6	3.920	-------	3.920	-------
7	4.573	4.573	-------	-------
8	5.226	-------	-------	5.226
9	5.879	-------	-------	-------
10	6.533	6.533	-------	-------
11	7.186	-------	7.186	-------
12	7.839	-------	-------	-------
13	8.492	8.492	-------	-------
14	9.146	-------	-------	-------
15	9.799	-------	-------	9.799
16	10.452	10.452	10.452	-------
17	11.105	-------	-------	-------
18	11.759	-------	-------	-------
19	12.412	12.412	-------	-------
20	13.065	-------	-------	-------

evaluated from

$$K_i = M_i/A_i\,\delta R_{n,i} \qquad (1)$$

In this equation, M_i is the rate of mass sublimation from the module, determined from the before- and after-run mass measurements and the corresponding run time; A_i is the exposed modular naphthalene surface area (A_i= WL= 6.0 cm x 1.5 cm); and $\delta R_{n,i}$ is equal to naphthalene vapor density at wall, R_{nw}, minus the naphthalene vapor density in bulk at module i, $R_{nb,i}$.

The naphthalene vapor density at wall was determined from Sogin's vapor pressure-temperature correlation [7] in conjunction with the ideal gas equation. To find R_{nb} at the axial midpoint of a module, a mass balance was performed on a control volume that encompassed the portion of the duct from the inlet up to the axial midpoint of the i th module. This resulted in the following expression:

$$R_{nb,i} = (1.5M_1 + 2\sum_{j=2}^{i-1} M_j + 1.5M_i)/Q_i \qquad (2)$$

where Q_i is the volumetric air-flow rate.

Next, the local mass transfer coefficients evaluated from Equation (1) were normalized through the definition of Sherwood number, so that for the i th module we have

$$Sh_i = K_i D_h/D \qquad (3)$$

In this equation, D is the diffusion coefficient and D_h, the hydraulic diameter, is equal to 2.4 cm. The diffusion coefficient was determined from the definition of Schmidt number Sc = μ/RD. For naphthalene ($C_{10}H_8$) diffusion in air, Sc= 2.5 [7].

Experimental Uncertainty

In every experimental work, there is a certain amount of uncertainty in the measured and calculated quantities. Therefore, it is necessary to declare the uncertainty of an experimental work so that the presented results can be used with confidence.

In the present study, the absolute uncertainty for independent quantities are: temperature ±0.25 C, time ±1 s, barometric pressure ±0.1 mm Hg, mass measurement ±0.1 mg, and linear dimension ±0.025 mm. Then for a typical run, we obtain the following relative uncertainties [8,9]:

$u_{Re} = \pm 3.15\%$, $u_{Sh} = \pm 3.0\%$

RESULTS AND DISCUSSION

The mass transfer coefficients in the entrance region of the duct for h/H = 0.5 and L/H = 1,3,5, and 7 are presented in Figures 2(a)-(d). In these figures, the abscissa is the dimensionless distance from the duct inlet, x/D_h, while the ordinate, $Sh_x/Sh_{fd,s}$, is the local Sherwood number divided by the fully-developed value of Sh for the smooth duct (without plates) at the same Reynolds number.

An overall examination of Figure 2 indicates that in all cases, the values of $Sh_x/Sh_{fd,s}$ are higher than unity, ranging from 1.34 (the 2nd data in Figure 2(c) at Re= 6974) to 11.51 (the 2nd data in Figure 2(a) at Re= 4800). This observation indicates that the presence of the plate blockages in a duct improves the transfer coefficients. The improvement is apparently due to an altered flow field which is substantially different from that in a smooth duct.

In an attempt to gain more understanding of the flow field, the authors conducted a series of flow visualization tests which are documented in Referene [10]. The flow visualization results revealed the presence of a flow separation and recirculating zone behind the plates, and often accompanied with impingement of fluid to the duct walls. We shall now try to relate the special features of the flow field such as flow separation, recirculation, and wall impingements, to the mass transfer results.

In this regard, it should be noted that the values of L/H indicate, in addition to the streamwise distance between the plates, the number of naphthalene-coated modules situated between each pair of neighboring plates. Therefore, the number of mass measurement sites (the number of data points) between each pair of neighboring plates in Figures 2(a), (b), (c), and (d) are respectively, 1,3,5, and 7. Clearly, as the number of interplate modules increases (i.e., at

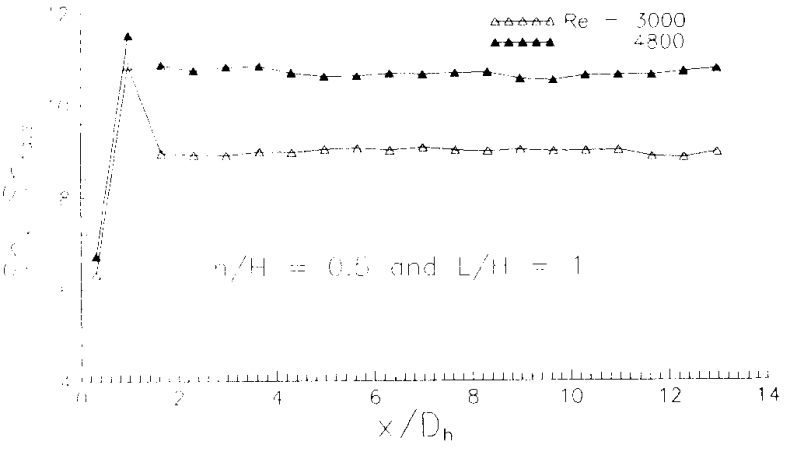

Figure 2(a). Axial distribution of Sherwood numbers for h/H= 0.5 & L/H= 1.

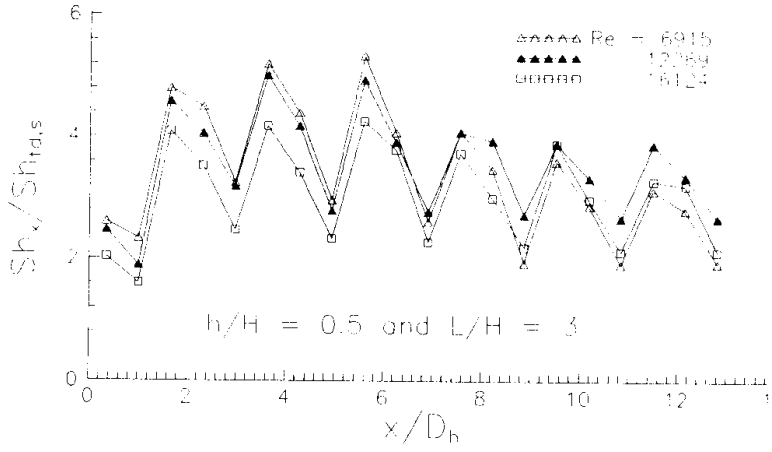

Figure 2(b). Axial distribution of Sherwood numbers for h/H= 0.5 & L/H= 3.

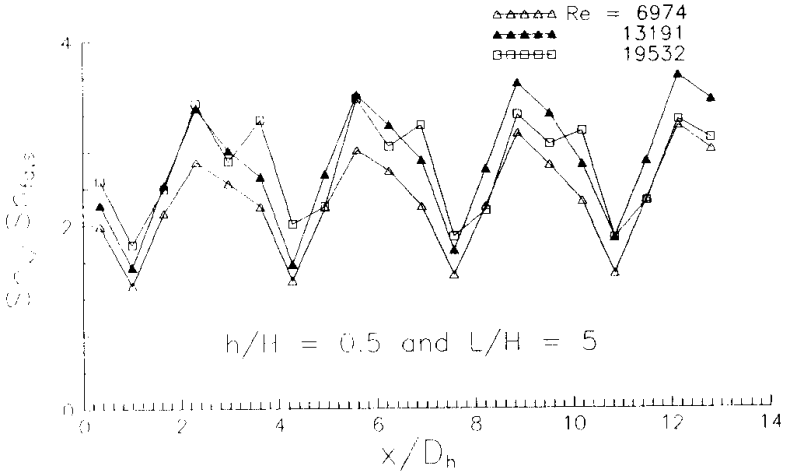

Figure 2(c). Axial distribution of Sherwood numbers for h/H= 0.5 & L/H= 5.

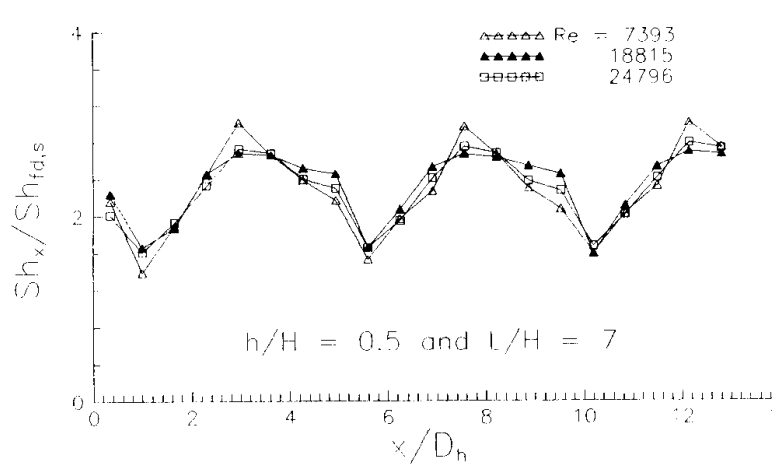

Figure 2(d). Axial distribution of Sherwood numbers for h/H= 0.5 & L/H= 7.

higher L/H), more information is obtained on the local variation of transfer coefficients.

Table 1 indicates that the first plate is always situated at $x/D_h = 0.653$ (for all values of L/H), while the axial positions of the other plates depend on L/H. In Figures 2(b)-(d), it is seen that the transfer coefficients just behind the plates, where the fluid is recirculating, are relatively low.

Further downstream, the local Sh number increases and reaches a local maximum point. In fact, this is nearly the point of reattachment where the fluid impinges on the duct wall. Downstream from this local maximum, the fluid tends to develop a boundary layer near the wall and the Sh number rapidly decreases. But the fluid soon encounters the next plate and the whole process of flow separation, recirculation, and wall impingement is repeated.

Attention is next turned to Figures 3(a)-(c) and 4(a)-(b). The general behavior of the families of curves in these figures is qualitatively similar to that mentioned earlier. The values of $Sh_x/Sh_{fd,s}$ range from 1.07 (the 2nd data in Figure 3(c) at Re= 39698) to 5.17 (the lst data in Figure 3(a) at Re = 10845) and are always higher than unity. It is further observed that as h/H is decreased or L/H is increased, the mass (heat) transfer coefficients generally diminish. These variations are closely related to the flow field and are interpreted by considering the fact that decreasing h/H or increasing L/H would, respectively, increase or decrease the extent of flow separation and recirculating zone behind the plates.

Figure 5 has been prepared to indicate the axial variation of mass (heat) transfer coefficient in a smooth duct. The smooth duct can be identified either by h/H = 0 or L/H = ∞. The latter identification of smooth duct is a useful notion, as it establishes a close and consistent link to the previous results. In this regard, it is seen that the Sherwood numbers consistently decrease as L/H goes from 1 to ∞.

The periodic nature of the results has been addressed in Figure 6. In this figure, the data corresponding to geometrically similar locations are shown by similar symbols. It is seen that similar symbols, i.e., open triangles, black triangles, etc., are located on nearly horizontal lines. The horizontality of these lines indicate that, in the downstream portion of the test duct, the Sherwood numbers at similar axial stations are equal and that the flow has attained a periodically fully-developed nature.

The periodically fully-developed Sherwood numbers

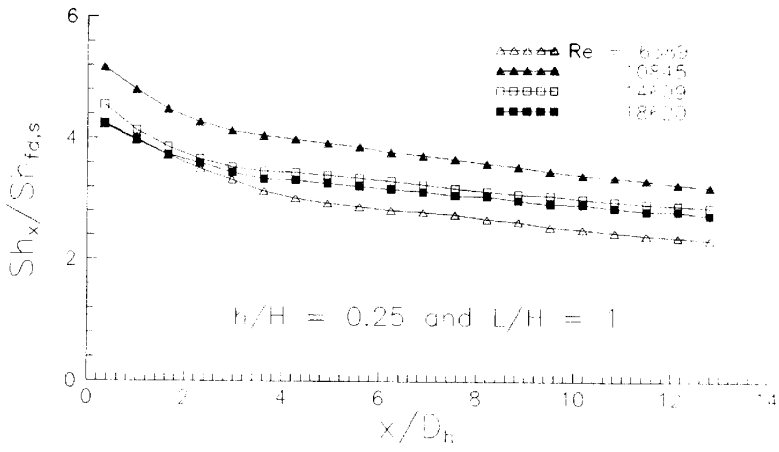

Figure 3(a). Axial distribution of Sherwood numbers for h/H= 0.25 & L/H= 1.

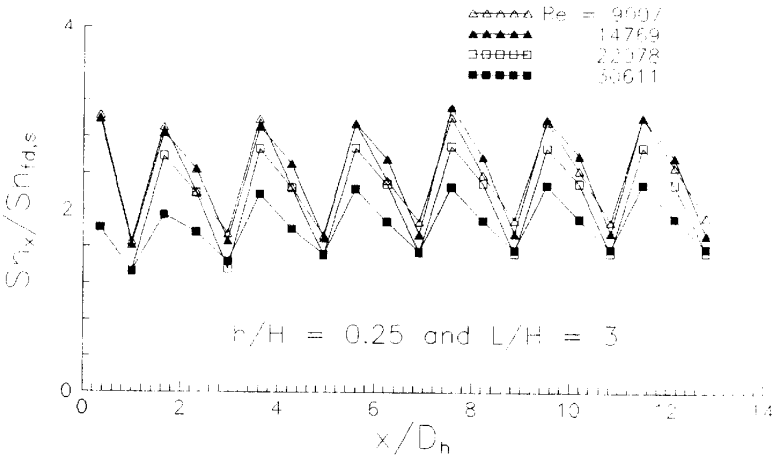

Figure 3(b). Axial distribution of Sherwood numbers for h/H= 0.25 & L/H= 3.

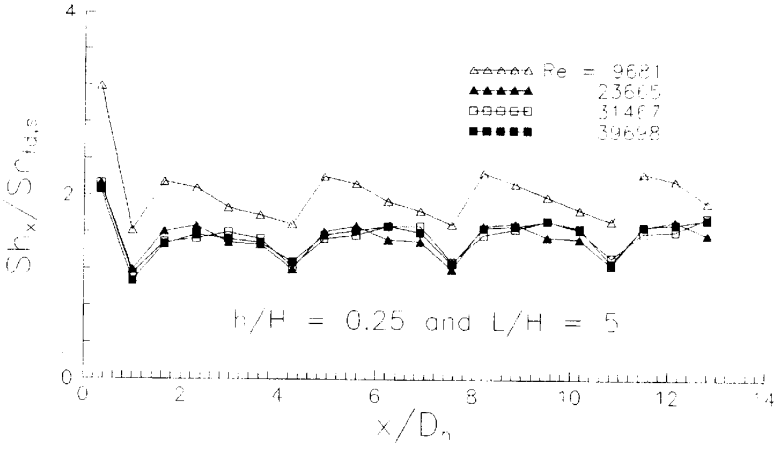

Figure 3(c). Axial distribution of Sherwood numbers for h/H= 0.25 & L/H= 5.

are presented in figures 7(a) - (c). The abscissa is Reynolds number based on mean fluid velocity through the duct cross-section and the hydraulic diameter D_h. It is seen that on a logarithmic scale, Sherwood numbers vary almost linearly with respect to Re. This suggests that the

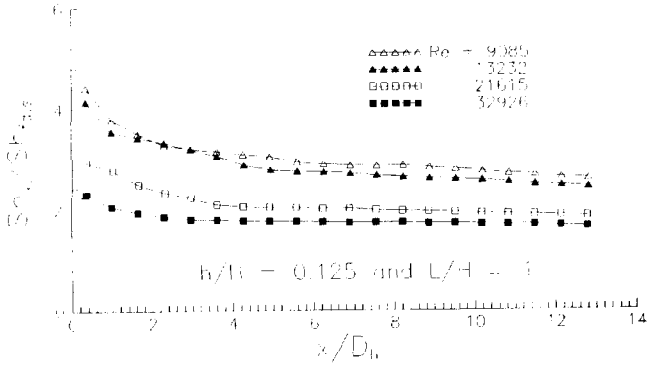

Figure 4(a). Axial distribution of Sherwood numbers for h/H= 0.125 & L/H= 1.

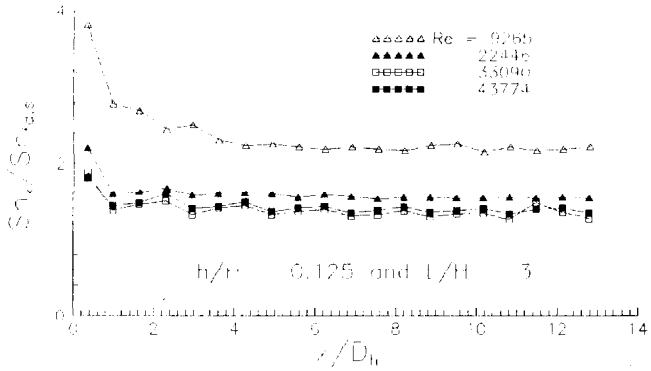

Figure 4(b). Axial distribution of Sherwood numbers for h/H= 0.125 & L/H= 3.

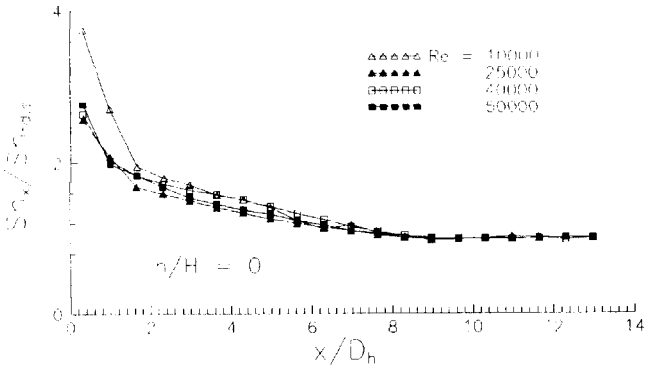

Figure 5. Axial distribution of Sherwood numbers for the smooth duct.

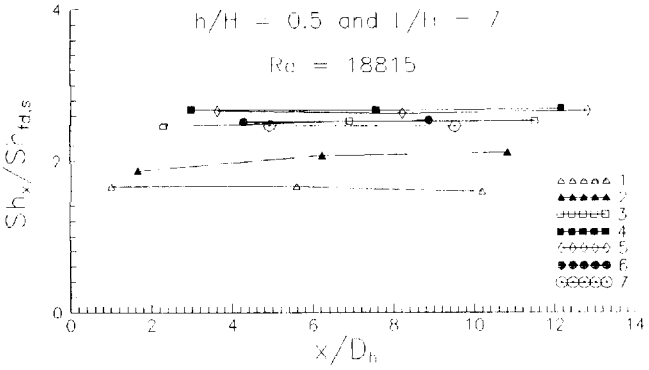

Figure 6. Sherwood numbers for similar axial stations.

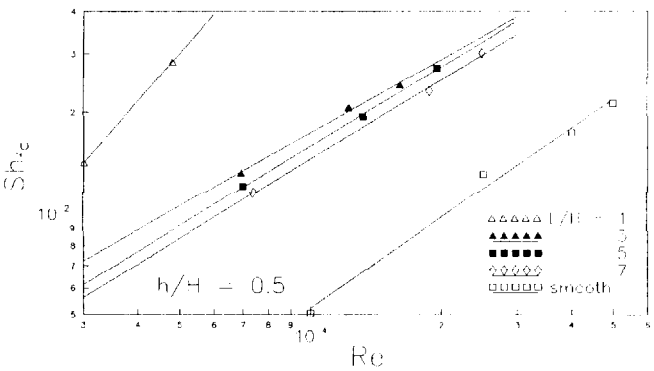

Figure 7(a). Periodically fully-developed Sherwood numbers for h/H= 0.5 & L/H= 1,3,5, and 7.

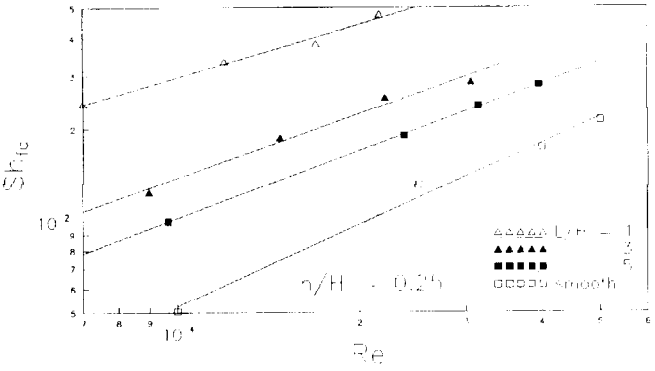

Figure 7(b). Periodically fully-developed Sherwood numbers for h/H= 0.25 & L/H= 1,3, and 5.

conventional duct flow correlation $Sh_{fd}= aRe^{b}$ also applies to the duct with plate blockages.

The solid lines seen in Figures 7(a)-(c) are the least-squares fits to the data. The coefficients of the power-law fits, i.e., a and b, were computed and are presented in Table 2.

An overall examination of the results indicates that the Sherwood numbers increase with Re, a trend observed for

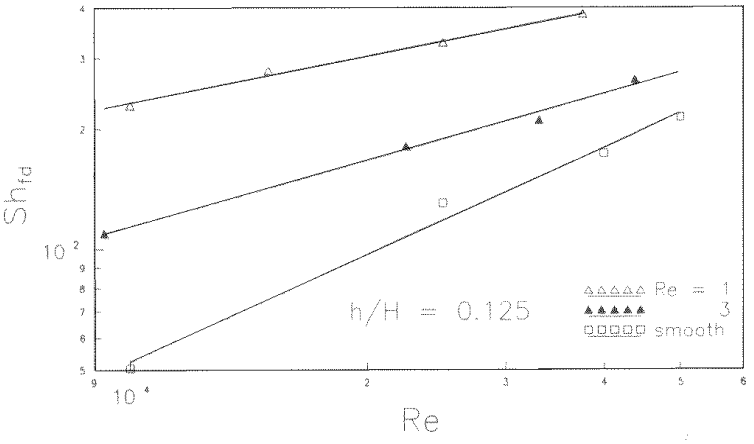

Figure 7(c). Periodically fully-developed Sherwood numbers for h/H= 0.125 & L/H= 1, and 3.

TABLE 2. Coefficients of the Least-Squares Fits to the Data

$Sh_{fd} = aRe^b$

h/H	L/H	a	b
0	∞	0.0148	0.887
0.125	1	6.7728	0.384
	3	0.7301	0.548
0.25	1	1.5368	0.572
	3	0.2182	0.700
	5	0.1173	0.735
0.5	1	0.000996	1.482
	3	0.2121	0.728
	5	0.1124	0.787
	7	0.1049	0.785

both smooth duct and the duct with plate blockages. Moreover, it is seen that in the case of the smooth duct, the dependence of Sh_{fd} on Re is somewhat stronger than other cases; an exception to this rule is the data corresponding to h/H= 0.5 and L/H= 1, which is believed to be in the transition region and is not considered a fully turbulent flow.

Another noteworthy feature of the flow, as is evident from Figures 7(a)-(c) and Table 2, is the effect of h/H and L/H on Sh_{fd}-Re correlation. At a fixed value of h/H, the slope of the Sh_{fd}-Re line (on log-log coordinates) generally indicates a slight increase with L/H. A similar trend is observed when L/H is held constant and h/H is varied. These variations are apparently due to a change in the flow field.

Derivation of Heat Transfer Coefficients

The mass transfer coefficients reported in this paper can be transformed into heat transfer results via the analogy between the two processes. In general, we can write the general correlation for heat transfer as

$$Nu = f(Re, Pr) \tag{4}$$

where Pr is the fluid Prandtl number. Due to the analogy, the mass transfer counterpart of this correlation is

$$Sh = f(Re, Sc) \tag{5}$$

where Sc is the Schmidt number and the function f is the same in both equations. Therefore, one could simply replace Sc in mass Equation (5) by Pr and obtain the heat Equation (4).

For example, if

$$Sh = a\,Re^b Sc^c \tag{6}$$

then

$$Nu = aRe^b Pr^c \tag{7}$$

After dividing Equation (7) by Equation (6), we have

$$Nu = (Pr/Sc)^c Sh \tag{8}$$

For the duct flow, it is normally assumed and often observed experimentally that c = 1/3 [11]. Substituting c= 1/3 and Sc = 2.5 in Equation (8),

$$Nu = (Pr/2.5)^{1/3}\,Sh \tag{9}$$

which is a convenient correlation for transforming Sh to Nu.

CONCLUDING REMARKS

This experimental work has revealed the heat (mass) transfer characteristics of turbulent flow in a square duct with wall-attached plate blockages. The experiments were carried out by mass transfer, and the analogy between heat and mass transfer provided a link between the two problems.

The results indicated that the presence of the plate

blockages always increased heat transfer relative to the smooth duct. The highest values were obtained at h/H= 0.5 and L/H= 1. As h/H was decreased or L/H increased, the degree of heat transfer enhancement diminished.

It was further found that transfer coefficients are generally low right behind the plates, but toward downstream they increase and attain a local maximum value. The location of this maximum value is postulated to be near the point where the separated flow impinges on the duct wall. These findings are supported by the flow visualization results of Reference [10].

NOMENCLATURE

A_i	mass transfer area per module, Equation (1)
C_D	discharge coefficient of orifice
D	diffusion coefficient, Equation (3)
D_h	hydraulic diameter of the duct, Equation (3)
H	height of the duct cross-section, Figure 1
h	plate height, Figure 1
K_i	mass transfer coefficient for module i, Equation (1)
L	streamwise plate spacing, Figure 1
M_i	permodule rate of mass sublimation, Equation (1), Equation (2)
Nu	Nusselt number, Equation (4)
Pr	Prandtl number, Equation (4)
Q_i	volumetric air flow rate at the axial location of module i, Equation (2)
R	density
$R_{nb,i}$	naphthalene vapor density in bulk at module i, Equation (2)
R_{nw}	naphthalene vapor density at wall
Re	Reynolds number, Equation, (4)
Sc	Schmidt number, Equation (5)
Sh	Sherwood number, Equation (5)
Sh_{fd}	fully-developed Sherwood number
$Sh_{fd,s}$	fully-developed Sherwood number for the smooth duct
Sh_i	Sherwood number for module i
Sh_x	Sherwood number at axial station x
W	duct width
x	axial coordinate (x= 0 at duct inlet)
μ	viscosity

REFERENCES

1. C. Berner, F. Durst and D.M. McEligot: "Flow around baffles", *ASME* paper 83-WA/HT-9 (1983).
2. E.M. Sparrow and K.P. Wachtler: "Transfer coefficients on the surfaces of a transverse plate situated in a duct flow", *Int. J. Heat Mass Transfer* 21, 761-767 (1978).
3. B.W. Webb and S. Ramadhyani: "Conjugate heat transfer in a channel with staggered ribs", *Int. J. Heat Mass Transfer* 28, 1679-1687 (1985).
4. K.M. Kelkar and S.V. Patankar: "Numerical prediction of flow and heat transfer in a parallel plate channel with staggered fins", *ASME J. Heat Transfer* 109, 25-30 (1987).
5. M. Molki and A.R. Mostoufizadeh: "Turbulent heat transfer in rectangular ducts with repeated-baffle blockages", *Int. J. Heat Mass Transfer* 32, 1491-1499 (1989).
6. E.R.G. Eckert: Analogies to heat transfer processes. In "Measurements in Heat Transfer" (Edited by E.R.G. Eckert and R.J. Goldstein), pp. 397-423, Hemisphere, Washington, DC (1976).
7. H.H. Sogin: "Sublimation from disks to air streams flowing normal to their surfaces", *Trans. Am. Soc. Mech. Engrs* 89, 61-69 (1958).
8. S.J. Kline: "The purposes of uncertainty analysis", *J. Fluids Engineering*, 107, 153-160 (1985).
9. R.B. Abernethy, R.P. Benedict and R.B. Dowdell: "ASME measurement uncertainty", *J. Fluids Engineering* 107, 161-164 (1985).
10. I. Mirzaee: "An experimental investigation of mass (heat) transfer coefficient in rectangular ducts with staggered plates", M. Sc. Thesis, Isfahan University of Technology, (1990).
11. J.P. Holman: "Heat transfer" (6th Edn), McGraw-Hill, New York (1986).